PROCEEDINGS OF SCIENCE

Applying the Worldvolume Hybrid Monte Carlo method to the finite-density complex ϕ^4 model and the Hubbard model[†]

Masafumi Fukuma[a,*] **and Yusuke Namekawa**[b,*]

[a] *Department of Physics, Kyoto University, Kyoto 606-8502, Japan*

[b] *Education and Research Center for Artificial Intelligence and Data Innovation, Hiroshima University, Hiroshima 739-8521, Japan*

E-mail: fukuma@gauge.scphys.kyoto-u.ac.jp, namekawa@hiroshima-u.ac.jp

The sign problem has been a major obstacle to first-principles calculations of important physical systems based on the Markov chain Monte Carlo algorithms. The Worldvolume Hybrid Monte Carlo method [1] is an efficient and low-cost algorithm to tame the sign problem that also eliminates the ergodicity problem inherent in algorithms based on Lefschetz thimbles. We apply the method to the complex ϕ^4 model at finite density as well as to the Hubbard model away from half filling. For the finite-density ϕ^4 model, we confirm that the computational cost is of $O(N^1)$ when using linear solvers such as BiCGStab (N: degrees of freedom), in contrast to the $O(N^3)$ cost of preceding Lefschetz thimble methods. For the Hubbard model, the computational cost increases due to the presence of the fermion determinant, but we argue that the cost will not exceed $O(N^2)$ with the use of pseudofermions.

The 40th International Symposium on Lattice Field Theory (Lattice 2023)
July 31st - August 4th, 2023
Fermi National Accelerator Laboratory

[†]Report No.: KUNS-2990

[*]Speaker

[§]This is a combined contribution of "Applying the Worldvolume Hybrid Monte Carlo method to dynamical fermion systems" (by M. Fukuma) and "Applying the Worldvolume Hybrid Monte Carlo method to the complex ϕ^4 theory at finite density" (by Y. Namekawa).

PoS(LATTICE2023)178

1. Introduction

In various important systems such as finite-density QCD, strongly correlated electron systems, frustrated spin systems, and the real-time dynamics of quantum many-body systems, the sign problem has been a major obstacle to first-principle calculations based on the Markov chain Monte Carlo method. Recently, several approaches that utilize the complexification of dynamical variables have been attracting attention. Among them, the Lefschetz thimble method [1–16] deforms the integration surface into the complex space. The deformation is designed such that the deformed surface approaches a union of Lefschetz thimbles, on each of which the imaginary part of the action is constant, and thus the sign problem is expected to be alleviated there. Although the potential barriers among thimbles cause the ergodicity problem, it can be controlled by tempering the system with respect to the deformation parameter, which is realized as the *tempered Lefschetz thimble method* in Ref. [10]. A drawback of this method is its high numerical cost of $O(N^3)$ (N: degrees of freedom) coming from the need to compute the Jacobian of the deformation. The *Worldvolume Hybrid Monte Carlo method* (WV-HMC method) [1, 15, 16] is introduced to solve this issue, where the HMC updates are performed on a continuous accumulation $\mathcal{R}$ of the deformed surfaces. The region $\mathcal{R}$ is named *worldvolume* à la string theory by regarding it as the orbit of the integration surface in the target space $\mathbb{C}^N$. The WV-HMC algorithm realizes the low computational cost because it does not require the explicit evaluation of the Jacobian in generating configurations.

In this article, we apply the WV-HMC method to the finite-density ϕ^4 model as well as to the Hubbard model away from half filling. For the former model, we show that the computational cost is $O(N^1)$ when using an iterative solver (such as BiCGStab) in linear inversions. For the Hubbard model, the computational cost increases due to the presence of the nonlocal fermion determinant, but we argue that the computational cost will not exceed $O(N^2)$ with the use of pseudofermions.

2. Worldvolume Hybrid Monte Carlo

Our aim is to evaluate the expectation values of observables $\mathcal{O}(x)$ defined by the path integral,

$$\langle \mathcal{O} \rangle \equiv \frac{\int_{\mathbb{R}^N} dx\, e^{-S(x)}\, \mathcal{O}(x)}{\int_{\mathbb{R}^N} dx\, e^{-S(x)}}, \tag{1}$$

where $\mathbb{R}^N = \{x\}$ is the configuration space and $S(x) \in \mathbb{C}$ the complex action. Since $e^{-S(x)}$ is complex-valued, it cannot be regarded as defining a probability density. A simple prescription is the naive reweighting method that uses the real part of the action for the probability density:

$$\langle \mathcal{O} \rangle = \frac{\int_{\mathbb{R}^N} dx\, e^{-\mathrm{Re}\, S(x)} \left(e^{-i\mathrm{Im}\, S(x)}\, \mathcal{O}(x) \right)}{\int_{\mathbb{R}^N} dx\, e^{-\mathrm{Re}\, S(x)}\, e^{-i\mathrm{Im}\, S(x)}}. \tag{2}$$

However, for systems with large degrees of freedom ($N \gg 1$), the numerator and the denominator become highly oscillatory integrals, which makes difficult numerical evaluations based on the Markov chain Monte Carlo method. In fact, statistical errors are hard to be made smaller than the means of order $e^{-O(N)}$.

A way to avoid this problem is to continuously deform the integral surface so that the sign problem is alleviated on the new integral surface Σ (see Fig. 1). In fact, when $e^{-S(z)}$ and $e^{-S(z)}\, \mathcal{O}(z)$

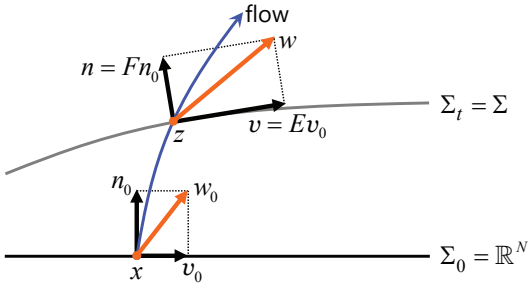

Figure 1: Deformation of the integration surface using the flow (figure taken from [16]).

are entire functions over $\mathbb{C}^N$ (as is the case for most models of interest), the integrals do not change under the deformation due to Cauchy's theorem, and the expectation value (1) can be written to

$$\langle O \rangle = \frac{\int_\Sigma dz\, e^{-S(z)}\, O(z)}{\int_\Sigma dz\, e^{-S(z)}}, \tag{3}$$

and thus the oscillatory behavior will be much relaxed if $\mathrm{Im}\, S(z)$ is almost constant on Σ. Such deformation can be realized by integrating the following flow equations:

$$\dot{z} = \overline{\partial S(z)}, \quad z|_{t=0} = x, \tag{4}$$

$$\dot{v} = \overline{H(z)v}, \quad v|_{t=0} = v_0, \tag{5}$$

$$\dot{n} = \overline{H(z)n}, \quad n|_{t=0} = n_0, \tag{6}$$

where $v \in T_z\Sigma_t$ ($n \in N_z\Sigma_t$) is the tangent (normal) vector, and $H_{ij}(z) \equiv \partial_i \partial_j S(z)$ is the Hessian matrix. This flow sends the original integration surface $\Sigma_0 = \mathbb{R}^N$ to a vicinity of a union of Lefschetz thimbles, on each of which $\mathrm{Im}\, S(z)$ is constant, and thus the oscillatory behavior is expected to be reduced on each connected component of Σ_t at a large flow time t. A Hybrid Monte Carlo algorithm on Σ_t with fixed t has been proposed in Refs. [13, 14], which is a HMC version of the generalized thimble method [9] and will be referred to as the GT-HMC method in this article.

Since both the numerator and the denominator in (3) do not depend on t, we can take averages over t with an arbitrary weight function $W(t)$,

$$\langle O \rangle = \frac{\int dt\, e^{-W(t)} \int_{\Sigma_t} dz\, e^{-S(z)}\, O(z)}{\int dt\, e^{-W(t)} \int_{\Sigma_t} dz\, e^{-S(z)}}. \tag{7}$$

We write this as a ratio of reweighted averages $\langle \cdots \rangle_{\mathcal{R}}$ on the *worldvolume* $\mathcal{R} \equiv \cup_t \Sigma_t = \{z_t(x) \,|\, t \in \mathbb{R},\, x \in \mathbb{R}^N\}$ (see Fig. 2):

$$\langle O \rangle = \frac{\langle \mathcal{F}(z)\, O(z) \rangle_{\mathcal{R}}}{\langle \mathcal{F}(z) \rangle_{\mathcal{R}}}, \tag{8}$$

$$\langle g(z) \rangle_{\mathcal{R}} \equiv \frac{\int_{\mathcal{R}} |dz|_{\mathcal{R}}\, e^{-V(z)}\, g(z)}{\int_{\mathcal{R}} |dz|_{\mathcal{R}}\, e^{-V(z)}}. \tag{9}$$

Here, $|dz|_{\mathcal{R}}$ is the invariant volume element of $\mathcal{R}$, $V(z) \equiv \mathrm{Re}\, S(z) + W(t(z))$ is the potential, and $\mathcal{F}(z)$ is the associated reweighting factor,

$$\mathcal{F}(z) \equiv \frac{e^{-S(z)-W(t(z))}\, dt\, dz}{e^{-V(z)}\, |dz|_{\mathcal{R}}} = \frac{dt\, dz}{|dz|_{\mathcal{R}}} e^{-i\, \mathrm{Im}\, S(z)}. \tag{10}$$

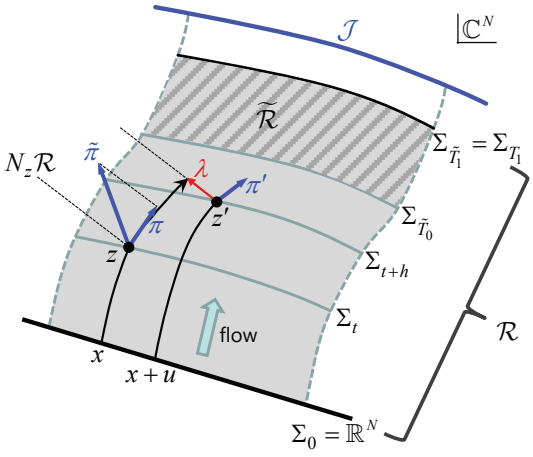

Figure 2: A molecular dynamics step on the worldvolume (figure taken from [16]).

The reweighted average (9) can be written to the phase space integral of the form

$$\langle g(z)\rangle_{\mathcal{R}} = \frac{\int_{T\Sigma} \hat{\omega}^{N+1}\, e^{-H(z,\pi)}\, g(z)}{\int_{T\Sigma} \hat{\omega}^{N+1}\, e^{-H(z,\pi)}}, \tag{11}$$

where $\pi \in T_z\mathcal{R}$ is the conjugate momentum, $\hat{\omega} \equiv \mathrm{Re}\, \overline{d\pi^i} dz^i$ is the symplectic form of the tangent bundle $T\mathcal{R} = \{(z,\pi) \mid z \in \mathcal{R},\ \pi \in T_z\mathcal{R}\}$, and $H(z,\pi)$ is the Hamiltonian of the form

$$H(z,\pi) = \frac{1}{2}\pi^\dagger\pi + V(z). \tag{12}$$

The molecular dynamics is given by RATTLE of the following form [1]:

$$\pi_{1/2} = \pi - \Delta s\, \overline{\partial V(z)} - \lambda/\Delta s, \tag{13}$$

$$z' = z + \Delta s\, \pi_{1/2}, \tag{14}$$

$$\pi' = \pi_{1/2} - \Delta s\, \overline{\partial V(z')} - \lambda'/\Delta s. \tag{15}$$

Here, the Lagrange multipliers $\lambda \in N_z\mathcal{R}$ and $\lambda' \in N_{z'}\mathcal{R}$ are determined such that $z' \in \mathcal{R}$ and $\pi' \in T_{z'}\mathcal{R}$, respectively. This transformation satisfies the reversibility and the symplecticity ($\hat{\omega}' = \hat{\omega}$) [and thus the volume preservation ($\hat{\omega}'^{N+1} = \hat{\omega}^{N+1}$)]. One can further show that it preserves the Hamiltonian to $O(\Delta s^2)$: $H(z',\pi') = H(z,\pi) + O(\Delta s^3)$.

The extent of the worldvolume $\mathcal{R}$ to the flow time direction can be effectively constrained to a finite interval $[T_0, T_1]$ by adjusting the functional form of $W(t)$, which we set as follows [16, 17]:

$$W(t) = \begin{cases} -\gamma(t-T_0) + c_0\left(e^{(t-T_0)^2/2d_0^2} - 1\right) & \text{for } t < T_0 \\ -\gamma(t-T_0) & \text{for } T_0 \le t \le T_1 \\ -\gamma(t-T_0) + c_1\left(e^{(t-T_1)^2/2d_1^2} - 1\right) & \text{for } t > T_1, \end{cases} \tag{16}$$

where γ is the tilt, c_0 (c_1) the height at T_0 (T_1), and d_0 (d_1) the penetration depth. These parameters are tuned so that configurations distribute almost uniformly over different flow times. The lower boundary T_0 is chosen such that the ergodicity is ensured on surfaces Σ_t with $t \sim T_0$, while the

upper boundary T_1 is taken to be large enough such that the oscillatory behavior is well relaxed at flow time $t \sim T_1$, which is judged by looking at the average reweighting factor $\langle \mathcal{F}(z) \rangle_{\Sigma_t}$ computed with the GT-HMC method. The signals of observables can be improved by using configurations retrieved from a subinterval $t \in [\tilde{T}_0, \tilde{T}_1]$ $(T_0 \le \tilde{T}_0 < \tilde{T}_1 \le T_1)$ [1, 15] (see Fig. 2). Here, $\tilde{T}_0$ works as a cutoff to eliminate configurations contaminated with the sign problem, and $\tilde{T}_1$ is for discarding configurations coming from a region in $\mathcal{R}$ which may be hard to sample because of its complicated geometry.

The computational cost of the GT-HMC and the WV-HMC algorithms is dominated by solving the linear equation $Aw_0 = w$ with $w_0 = v_0 + n_0$, $w = v + n$ (see Fig. 1). Direct solvers following the computation of all the matrix elements of A require the computational cost of $O(N^3)$. On the other hand, for iterative solvers such as BiCGStab, the multiplication of A can be replaced by the integration of the vector flow equations (5) and (6) [18]. Thus, if the convergence of iteration depends on the system size only weakly, the computational cost is expected to be reduced from $O(N^3)$ to $O(N)$ when the Hessian matrix is sparse (as is the case for the finite-density ϕ^4 model). If the Hessian is nonlocal (as is the case of the Hubbard model in a bosonized form with the fermion determinant), the computational cost increases, but we argue that it may not exceed $O(N^2)$ if we use pseudofermions from the beginning.

3. Application to a field theory with a local action

We apply the WV-HMC method to the finite-density ϕ^4 model as a typical example of a local field theory whose Hessian matrix $H_{ij} = \partial_i \partial_j S$ is sparse.

Following the strategy given in Sect. 2, we first use the GT-HMC method to determine the upper flow time T_1 by investigating whether the average reweighting factor $\langle \mathcal{F} \rangle_{\Sigma_{T_1}}$ is consistent to being nonzero within statistical errors. Then, setting $T_0 = 0$, we generate configurations on $\mathcal{R}$ using WV-HMC with this flow time interval $[T_0, T_1]$ and make measurements of observables.

We also investigate the computational cost scaling for this model. We here employ GT-HMC (instead of WV-HMC) because one can make a more precise statement about the scaling when the flow time is fixed. Since most of the flow times t of WV-HMC are smaller than the flow time set in GT-HMC $(= T_1)$, the computation time for GT-HMC can be regarded as giving an upper bound on that for WV-HMC.

For the weight function $W(t)$ [see Eq. (16)], we set the parameters to $\gamma = 20 - 100$, $c_0 = c_1 = 1$, $d_0 = d_1 = 0.02$ for 4^4 lattice, and $\gamma = 160 - 180$, $c_0 = c_1 = 1$, $d_0 = d_1 = 0.02$ for 6^4 lattice. For comparison, we also perform simulations using the complex Langevin method, which avoids the wrong convergence for the current model parameters. A further study of the finite-density ϕ^4 model will be made in Ref. [17].

3.1 Complex scalar ϕ^4 model at finite density

The complex ϕ^4 scalar model at finite density has been used as a testbed of methods towards solving the sign problem [4, 5, 19–24]. Its continuum action in four dimensions is given by

$$S_{\text{cont}}[\phi] \equiv \int d^4x \big[|\partial_\nu \phi|^2 + m^2 |\phi|^2 + \lambda |\phi|^4 + \mu(\bar{\phi}(\partial_0 \phi) + (\partial_0 \bar{\phi})\phi) \big], \tag{17}$$

where m is the mass, λ the self-coupling, and μ the chemical potential. The discretized action in lattice units [19] is

$$S(\phi) \equiv \sum_x \Big[-\sum_{\nu=0}^{3} \left(\bar{\phi}_{x+\nu}\, e^{+\mu\delta_{\nu 0}} \phi_x + \bar{\phi}_x\, e^{-\mu\delta_{\nu 0}} \phi_{x+\nu} \right) + (8+m^2)\bar{\phi}_x\phi_x + \lambda(\bar{\phi}_x\phi_x)^2 \Big]. \tag{18}$$

The number density operator n is defined by

$$n(\phi) \equiv -\frac{1}{N_s^3 N_t} \frac{\partial S(\phi;\mu)}{\partial \mu}, \tag{19}$$

where $N_s\,(N_t)$ is the size of the spatial (temporal) extent of the lattice.

We set the model parameters to $m = 0.1$, $\lambda = 1$ with $\mu = 0.40 - 0.90$ for 4^4 lattice and $\mu = 0.65 - 0.75$ for 6^4 lattice. These parameters cover the region suffering from the severe sign problem, which is the vicinity of the critical chemical potential ($\mu_c \sim 0.7$) where the number density starts to grow from zero. Figure 3 displays the average phase factors obtained with the naive reweighting method (2). They are consistent with zero in $\mu = 0.60 - 0.80$, which shows the sign problem is actually severe for this parameter region.

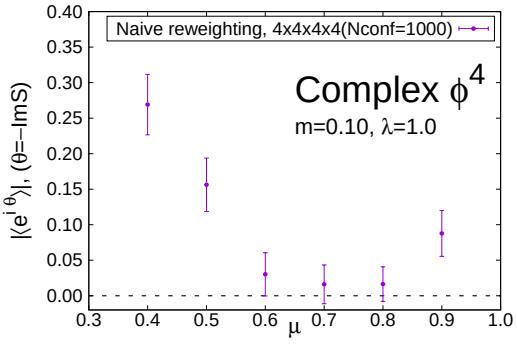

Figure 3: Average phase factor with the naive reweighting method.

3.2 Simulations

3.2.1 Determination of T_1

Figure 4 shows the T-dependence of the average reweighing factor obtained with the GT-HMC method. We see that it takes nonzero values at $T = 0.08$ for $\mu = 0.40 - 0.90$. Based on this result, we set $T_1 = 0.08$ in the WV-HMC simulations.

3.2.2 Configuration generation and measurement

Figure 5 is a set of the histograms of the flow time t with the tuned $W(t)$ [Eq. (16)], showing that the flow times distribute almost uniformly over the entire region $[T_0, T_1]$. The average reweighting factors (10) are plotted in Fig. 6, which confirms that they are nonzero within two standard deviations throughout the simulation parameter region.

We measure the number density n [Eq. (19)] and the field squared $|\phi|^2$. Figure 7 shows the $\tilde{T}_0$-dependence of $\langle n \rangle$. The statistical errors decrease as we increase $\tilde{T}_0$, reflecting the sign problem

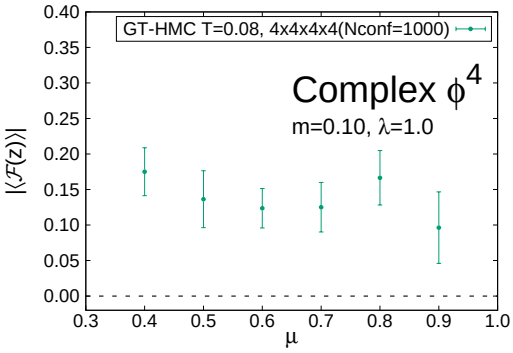

Figure 4: Average phase factor with the GT-HMC method.

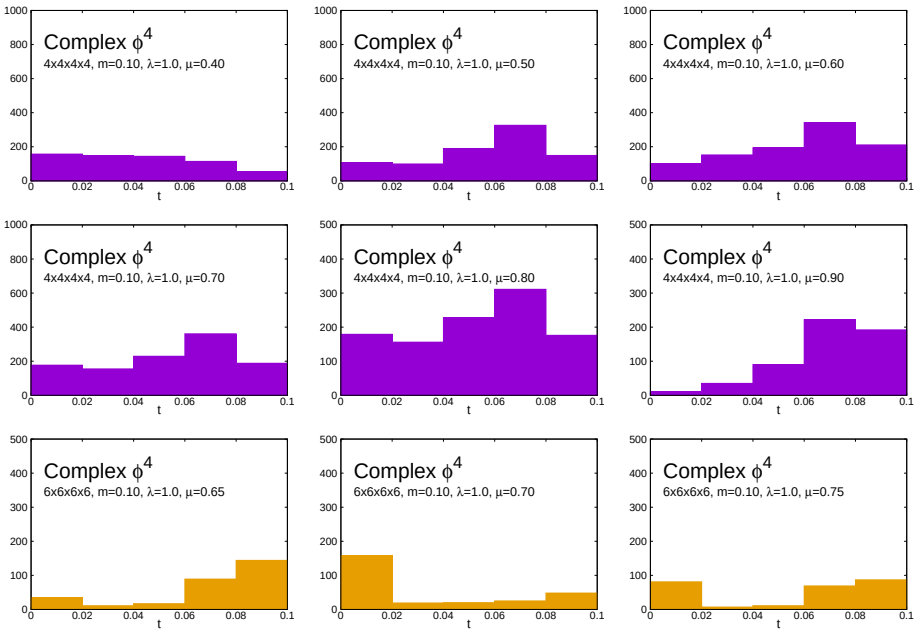

Figure 5: Histogram of the flow times t (WV-HMC).

is reduced along the flow. From this figure and the observation that $\tilde{T}_1$-dependence is mild, we set $\tilde{T}_0 = 0.03$ and $\tilde{T}_1 = T_1 = 0.08$ in the statistical analysis. Figure 8 shows the obtained results for $\langle n \rangle$ and $\langle |\phi|^2 \rangle$. They agree with those obtained with the complex Langevin method, which we confirm is free from the wrong convergence for these model parameters.[1]

3.2.3 Computational cost scaling

In Fig. 9, we plot the elapsed computer times of the BiCGStab and the RATTLE parts in the GT-HMC method. These elapsed times are measured on 256 nodes (8192 cores) of the supercomputer "Fugaku". We confirm that the elapsed time shows the $O(N^1)$ scaling in the region $N > 5 \times 10^7$.

[1]The data of the tensor renormalization group are taken from Ref. [24]. A discrepancy from other results may be due to the small D_{cut} (= 50) [26].

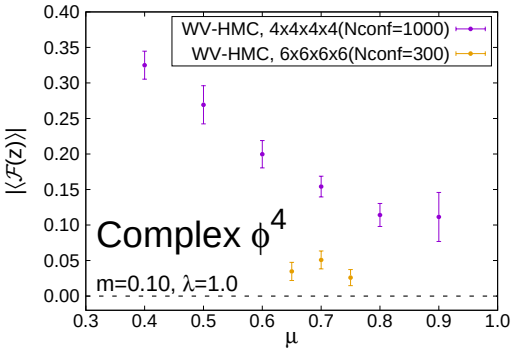

Figure 6: Average reweighting factors.

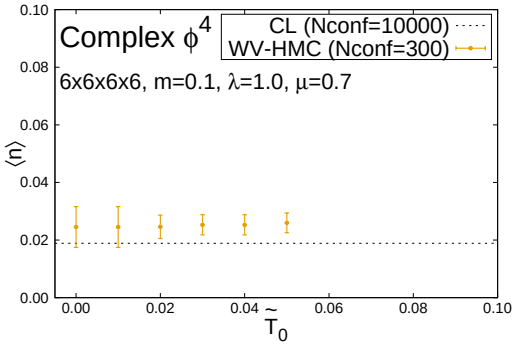

Figure 7: $\tilde{T}_0$-dependence of number density.

The data at small N deviate from the $O(N^1)$ scaling, because the elapsed time is dominated by the communication time there.

4. Application to a field theory with the fermion determinant

In this section, we consider the application of the WV-HMC algorithm to dynamical fermion systems. As a simple example we take the Hubbard model away from half filling, whose basic structure is similar to that of finite-density QCD.

4.1 Hubbard model

The Hamiltonian of the d-dimensional Hubbard model is given by

$$H = -\kappa \sum_{\langle \mathbf{x},\mathbf{y} \rangle} \sum_{\sigma} c^{\dagger}_{\mathbf{x},\sigma} c_{\mathbf{y},\sigma} - \mu \sum_{\mathbf{x}} (n_{\mathbf{x},\uparrow} + n_{\mathbf{x},\downarrow}) + U \sum_{\mathbf{x}} n_{\mathbf{x},\uparrow} n_{\mathbf{x},\downarrow}, \tag{20}$$

where κ is the hopping parameter, μ the chemical potential, and U the on-site repulsion strength. The symbol $\langle \mathbf{x}, \mathbf{y} \rangle$ represents the nearest-neighbor sites on a d-dimensional periodic lattice of size N_s^d, and $n_{\mathbf{x},\sigma} \equiv c^{\dagger}_{\mathbf{x},\sigma} c_{\mathbf{x},\sigma}$ is the number operator. The $(1+d)$-dimensional Euclid action after the Trotter decomposition ($\beta = N_t \epsilon$) and the Hubbard-Stratonovich transformation takes the following

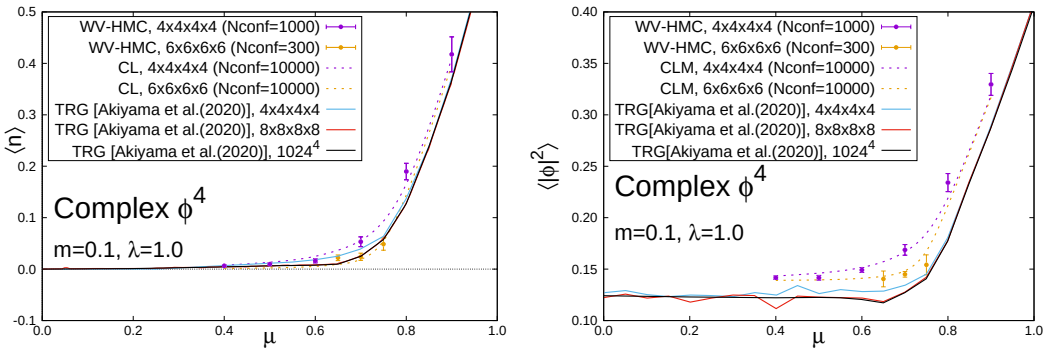

Figure 8: Number density and field squared, in comparison with the complex Langevin and the tensor renormalization group results [24].

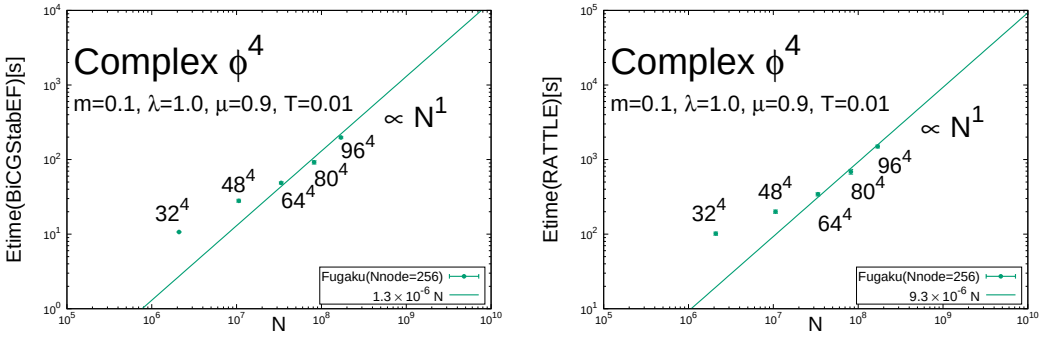

Figure 9: Elapsed time scaling of the BiCGStab part (left panel) and the RATTLE part (right panel) in the GT-HMC method as functions of N (degrees of freedom).

form with two-flavor fermions $\psi_x = (\psi_{x,\uparrow}, \psi_{x,\downarrow})^T$:

$$S(A,\bar{\psi},\psi) = \frac{1}{2}\sum_x A_x^2 + \sum_x \bar{\psi}_x (D(A)\psi)_x \,. \tag{21}$$

Here, $x = (x_0, \mathbf{x})$ is $(1+d)$-dimensional coordinates, A_x is the Hubbard-Stratonovich field, and the fermion operator $D(A)$ is given by

$$(D(A)\psi)_x = e^{\epsilon(\mu+U/2)+i\sqrt{\epsilon U}A_x}\,\psi_x - \psi_{x+\hat{0}} + \epsilon\kappa \sum_{j=1}^{d} (\psi_{x+j} + \psi_{x-j}) \,. \tag{22}$$

We impose the periodic (anti-periodic) boundary condition in the spatial (temporal) direction. The ground canonical partition function is then given by

$$Z = \int (dA\, d\bar{\psi}\, d\psi)\, e^{-(1/2)A^TA - \bar{\psi}D(A)\psi} = \int (dA)\, e^{-(1/2)A^TA} \left(\det D(A)\right)^2 . \tag{23}$$

In addition to this "chiral form," the partition function can also be written in a "nonchiral form,"

$$Z = \int (dA)\, e^{-(1/2)A^TA}\, \det D'_+(A)\, \det D'_-(A) \tag{24}$$

with

$$(D'_{\pm}(A)\psi)_x \equiv e^{\pm\epsilon(\mu-U/2)\pm i\sqrt{\epsilon U}A_x}\,\psi_x - \psi_{x\pm\hat{0}} + \epsilon\kappa\sum_{j=1}^{d}(\psi_{x+j}+\psi_{x-j})\,. \tag{25}$$

Note that the latter gives a positive (semi-)definite Boltzmann weight at the half filling ($\mu = U/2$), and is useful when investigating parameters near half filling.

There can be two approaches to dealing with the fermion determinant. One is to use A as the only dynamical variable and consider the action $S(A) = (1/2)A^TA - 2\,\mathrm{tr}\ln\det D(A)$ (or $S'(A) = (1/2)A^TA - \mathrm{tr}\ln\det D'_+(A) - \mathrm{tr}\ln\det D'_-(A)$). In this case, the numerical cost of RATTLE is $O(N^3)$ with $N = N_t \times N_s^d$. The other is to introduce pseudofermions and use iterative solvers to invert the fermion matrix D (or $D'_\pm$). In this case, the numerical cost is expected to be $O(N^2)$ at most if the convergence of iteration does not depend on the system size significantly. We use the first approach when investigating the sign problem, while we use the second when discussing the numerical cost scaling.

4.2 Existence of the sign problem

In Fig. 10, we plot the average phase factor of the naive reweighting method. It is consistent with zero in 2σ on $N_t \times N_s = 24 \times 6$ lattice for the parameter region $-4 \le \mu \le 8$ except near half filling, indicating that the sign problem is severe there.

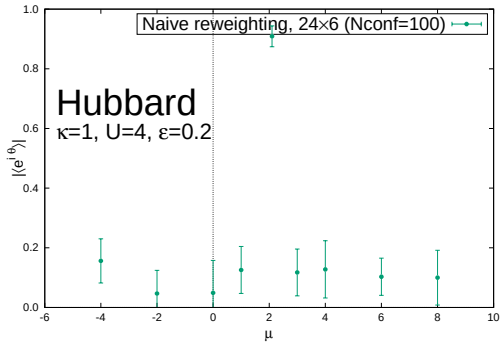

Figure 10: Average phase factor with the naive reweighting method.

In contrast to the finite-density ϕ^4 model, the complex Langevin method suffers from the singular drift problem, as shown in Fig. 11 (left panel). The drift histogram of the fermion part is plotted in Fig. 11 (right panel) and exhibits power-law tails, which violate the justification criterion [25].

4.3 Computational cost scaling

We investigate the computational cost scaling for the GT-HMC method when using pseudo-fermions. The scaling is expected to be $O(N^2)$ if the convergence of the Newton method in RATTLE with iterative solvers depends on the system size only weakly.

In Fig. 12, we show the elapsed computer times of the BiCGStab and the molecular dynamics parts in GT-HMC. We observe that the scaling is shifting from $O(N^3)$ to $O(N^2)$ at larger N.

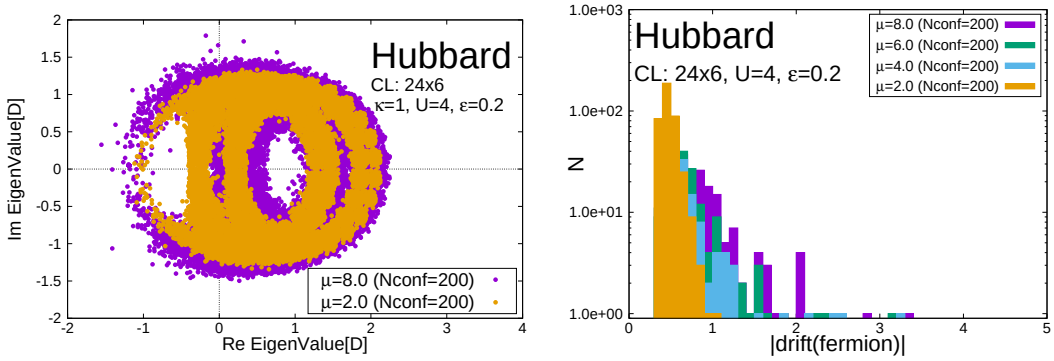

Figure 11: Eigenvalue distribution of the fermion matrix D (left panel), and fermion drift histogram (right panel) with the complex Langevin method.

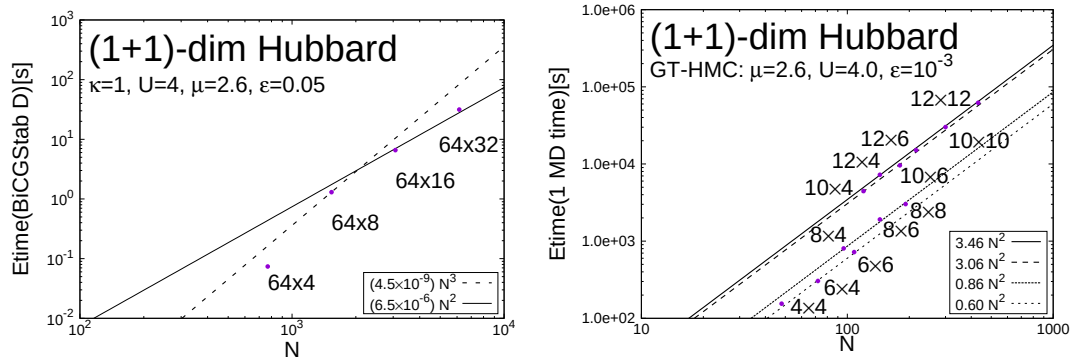

Figure 12: Elapsed time scaling of the BiCGStab part (left panel) and the molecular dynamics part (right panel) with respect to N (degrees of freedom).

5. Conclusion

In this article, we have applied the WV-HMC algorithm [1] to the ϕ^4 model at finite density as well as to the Hubbard model away from half filling. For the finite-density ϕ^4 model, we confirmed that the obtained results for $\langle n \rangle$ and $\langle |\phi|^2 \rangle$ agree with those of the complex Langevin method (free from the wrong convergence for this case). We also estimated the computational cost of both models by using the GT-HMC method. For the finite-density ϕ^4 model we found the expected $O(N^1)$ scaling in the elapsed time for configuration generation, while for the Hubbard model we argue that the computational cost does not exceed $O(N^2)$ if one uses pseudofermions in treating the fermion determinant.

In parallel to the study of these models, we are applying the WV-HMC algorithm to other systems that have serious sign problems, such as finite density QCD, strongly correlated electron systems, frustrated spin systems, and the real-time dynamics of quantum many body systems. The study of these models will be reported elsewhere.

Acknowledgments

The authors thank Shinichiro Akiyama, Sinya Aoki, Ken-Ichi Ishikawa, Daisuke Kadoh, Issaku Kanamori, Yoshio Kikukawa, and Nobuyuki Matsumoto for valuable discussions. This work was partially supported by JSPS KAKENHI (Grant Numbers 20H01900, 21K03553, 23H00112, 23H04506) and by MEXT as "Program for Promoting Researches on the Supercomputer Fugaku" (Simulation for basic science: approaching the new quantum era, JPMXP1020230411) and used computational resources of the supercomputer Fugaku provided by the RIKEN Center for Computational Science (Project ID: hp230207).

References

[1] M. Fukuma and N. Matsumoto, "Worldvolume approach to the tempered Lefschetz thimble method," PTEP **2021**, no.2, 023B08 (2021) [arXiv:2012.08468 [hep-lat]].

[2] E. Witten, "Analytic continuation of Chern-Simons theory," AMS/IP Stud. Adv. Math. **50**, 347-446 (2011) [arXiv:1001.2933 [hep-th]].

[3] M. Cristoforetti, F. Di Renzo and L. Scorzato, "New approach to the sign problem in quantum field theories: High density QCD on a Lefschetz thimble," Phys. Rev. D **86**, 074506 (2012) [arXiv:1205.3996 [hep-lat]].

[4] M. Cristoforetti, F. Di Renzo, A. Mukherjee and L. Scorzato, "Monte Carlo simulations on the Lefschetz thimble: Taming the sign problem," Phys. Rev. D **88**, no. 5, 051501(R) (2013) [arXiv:1303.7204 [hep-lat]].

[5] H. Fujii, D. Honda, M. Kato, Y. Kikukawa, S. Komatsu and T. Sano, "Hybrid Monte Carlo on Lefschetz thimbles - A study of the residual sign problem," JHEP **1310**, 147 (2013) [arXiv:1309.4371 [hep-lat]].

[6] H. Fujii, S. Kamata and Y. Kikukawa, "Lefschetz thimble structure in one-dimensional lattice Thirring model at finite density," JHEP **11**, 078 (2015) [erratum: JHEP **02**, 036 (2016)] [arXiv:1509.08176 [hep-lat]].

[7] H. Fujii, S. Kamata and Y. Kikukawa, "Monte Carlo study of Lefschetz thimble structure in one-dimensional Thirring model at finite density," JHEP **12**, 125 (2015) [erratum: JHEP **09**, 172 (2016)] [arXiv:1509.09141 [hep-lat]].

[8] A. Alexandru, G. Başar and P. Bedaque, "Monte Carlo algorithm for simulating fermions on Lefschetz thimbles," Phys. Rev. D **93**, no. 1, 014504 (2016) [arXiv:1510.03258 [hep-lat]].

[9] A. Alexandru, G. Başar, P. F. Bedaque, G. W. Ridgway and N. C. Warrington, "Sign problem and Monte Carlo calculations beyond Lefschetz thimbles," JHEP **1605**, 053 (2016) [arXiv:1512.08764 [hep-lat]].

[10] M. Fukuma and N. Umeda, "Parallel tempering algorithm for integration over Lefschetz thimbles," PTEP **2017**, no. 7, 073B01 (2017) [arXiv:1703.00861 [hep-lat]].

[11] A. Alexandru, G. Başar, P. F. Bedaque and N. C. Warrington, "Tempered transitions between thimbles," Phys. Rev. D **96**, no. 3, 034513 (2017) [arXiv:1703.02414 [hep-lat]].

[12] M. Fukuma, N. Matsumoto and N. Umeda, "Applying the tempered Lefschetz thimble method to the Hubbard model away from half filling," Phys. Rev. D **100**, no. 11, 114510 (2019) [arXiv:1906.04243 [cond-mat.str-el]].

[13] A. Alexandru, "Improved algorithms for generalized thimble method," talk at the 37th international conference on lattice field theory, Wuhan, 2019.

[14] M. Fukuma, N. Matsumoto and N. Umeda, "Implementation of the HMC algorithm on the tempered Lefschetz thimble method," [arXiv:1912.13303 [hep-lat]].

[15] M. Fukuma, N. Matsumoto and Y. Namekawa, "Statistical analysis method for the worldvolume hybrid Monte Carlo algorithm," PTEP **2021**, no.12, 123B02 (2021) [arXiv:2107.06858 [hep-lat]].

[16] M. Fukuma, "Simplified algorithm for the Worldvolume HMC and the Generalized-thimble HMC," [arXiv:2311.10663 [hep-lat]].

[17] M. Fukuma and Y. Namekawa, "Applying the Worldvolume Hybrid Monte Carlo method to the complex scalar field theory at finite density," in preparation.

[18] A. Alexandru, G. Basar, P. F. Bedaque and G. W. Ridgway, Phys. Rev. D **95**, no.11, 114501 (2017) [arXiv:1704.06404 [hep-lat]].

[19] G. Aarts, "Can stochastic quantization evade the sign problem? The relativistic Bose gas at finite chemical potential," Phys. Rev. Lett. **102**, 131601 (2009) [arXiv:0810.2089 [hep-lat]].

[20] C. Gattringer and T. Kloiber, "Lattice study of the Silver Blaze phenomenon for a charged scalar ϕ^4 field," Nucl. Phys. B **869**, 56-73 (2013) [arXiv:1206.2954 [hep-lat]].

[21] O. Orasch and C. Gattringer, "Canonical simulations with worldlines: An exploratory study in ϕ^4_2 lattice field theory," Int. J. Mod. Phys. A **33**, no.01, 1850010 (2018) [arXiv:1708.02817 [hep-lat]].

[22] Y. Mori, K. Kashiwa and A. Ohnishi, "Application of a neural network to the sign problem via the path optimization method," PTEP **2018**, no.2, 023B04 (2018) [arXiv:1709.03208 [hep-lat]].

[23] D. Kadoh, Y. Kuramashi, Y. Nakamura, R. Sakai, S. Takeda and Y. Yoshimura, JHEP **02**, 161 (2020) doi:10.1007/JHEP02(2020)161 [arXiv:1912.13092 [hep-lat]].

[24] S. Akiyama, D. Kadoh, Y. Kuramashi, T. Yamashita and Y. Yoshimura, "Tensor renormalization group approach to four-dimensional complex ϕ^4 theory at finite density," JHEP **09**, 177 (2020) [arXiv:2005.04645 [hep-lat]].

[25] K. Nagata, J. Nishimura and S. Shimasaki, "Argument for justification of the complex Langevin method and the condition for correct convergence," Phys. Rev. D **94**, no.11, 114515 (2016) [arXiv:1606.07627 [hep-lat]].

[26] S. Akiyama, D. Kadoh, Y. Kuramashi, T. Yamashita and Y. Yoshimura, private communication.